BOLLETTINO DI GEOFISICA TEORICA ED APPLICATA VOL. 38, N. 3-4, pp. 229-245; SEP.-DEC. 1997

On tidal analyses with measurement errors

E. MARONE [1] and A. R. DE MESQUITA [2]

[1] *Centro de Estudos do Mar, Paraná, Brazil*
[2] *Instituto Oceanografico, São Paulo, Brazil*

(Received December 10, 1992; accepted June 15, 1995)

Abstract. This work presents an approach to estimate measurement errors in tidal analysis. Independent methods deductive and inductive were used. The results showed good agreement. Theoretically deduced results were compared with computer assisted proofs. Both cases showed that measurement errors cannot be ignored but must be considered before deciding to accept or reject the determined tidal constituents. A real sea-level record from Cananéia, Brazil, assumed as an error free series (EFS) was used, from which synthetic series were obtained by the addition of statistically distributed known errors. Fourier analysis was applied to the series, taken as following a mixed model, and the results were compared. It was possible to show that measurement errors in amplitudes, due to the recording device, may add $\pm\sqrt{2\sigma}$ to each tidal constituent, where σ is the measurement error' standard deviation, which degrades the determination of the tidal constituent amplitudes. All tidal constituents smaller than that value must be rejected. Errors due to clock mechanisms generate spectral spreading of energy, by aliasing to high frequencies and by dispersion in both spectral directions. A method based on Fourier Interpolation was adequate to recover the original series spoiled by acceleration or deceleration of the tide gauge's clock. Added timing errors distributed in a jittered sampling manner were reckoned to minimize aliasing, improving the analysis of amplitudes, but not of the phases.

1. Introduction

Classical approaches to estimate tidal constituents (e. g., Munk and Cartwright, 1966; Franco and Rock, 1974; Mosetti and Purga, 1985) were able to show the uncertainties and "variability" of tidal constants, due to various causes. However the uncertainties were handled in a general form as the "noise" of the system. Sometimes, measurement errors were supposed to "be eliminated" by filtering (Zetler et al., 1979), and sometimes they were assumed negligible.

Corresponding author: E. Marone; Centro de Estudos do Mar, CEP, 83255-000 Paraná, PR, Brazil; e-mail: maroneed@aica.cem.ufpr.br

Munk and Cartwright (1966) were able to calculate the probability distribution of the transfer function in the Response Method, using parametric analysis. On the basis of this distribution, the rejection criteria for amplitude and phases of tidal constituents were proposed.

Franco and Rock (1974), using a non-parametric analysis, arrived at approximately the same probability distribution for the tidal constituents, and based on that characteristic, they also proposed a criterion for rejecting, or eliminating the weaker lines of the spectrum.

Gutiérrez et al. (1981) showed that tidal constants were not so "constant", and they related the variabilities to several causes, such as meteorological and other non-linear effects, but did not consider the measurement errors.

Mosetti (1983) showed that the tidal harmonic constants should be treated like random variables and, in consequence, a new method of analysis can then be used. In this way, he applied a Kalman filter estimate of the tidal harmonic constants, improving the results by the elimination of some variabilities present in the sea-level record.

Marone (1991) identified three kinds of errors in tidal analysis: modelling errors, due to the mathematical model used to fit the tidal data; methodological errors, caused by the use of stochastic estimation of the model parameters; and measurement errors, due to the measurement device, data reduction, and processing method.

In the first two approaches, it was assumed that the limiting factor in the determination of the precision of any tidal analysis is not the accuracy of the measurements, but the amount of noise present in the record, due to several types of interference (Cartwright and Amin, 1986).

1.1. The measurement errors

The observed sea-level height at instant t, X_t, in a mixed model can be represented by

$$X_t = X'_t + \varepsilon_t, \tag{1}$$

where

$$X'_t = \sum_{i=1}^{K} H_i \cos\left(\omega_i t + \phi_i\right) \tag{2}$$

with $i = 1,..., K$, $K=N/2$, and ε_t is pure random process independent of the phases ϕ_i and the frequencies ω_i, having $E(\varepsilon_t = 0$, $E(\varepsilon_t^2)= \sigma_t^2$ and a continuous uniform spectrum. Eq. (1) represents a mixed model (Priestley, 1981), where H_i are the amplitudes, ω_i the frequencies and ϕ_i the phases of the harmonic constituents.

For tides, the frequencies ω_i are known a priori, and given N+1 observations X_0, X_1,..., X_N, in the interval [0,T], with the sampling interval $\Delta_t = T/N$, the problem of estimating the amplitudes H_i and phases ϕ_i is solved by minimizing the expression

$$\varepsilon_a = 1/(N+1) \sum_{t=0}^{N+1} \left\{ X_t - \sum_{i=1}^{K} \left[A'_i \cos\left(\omega_i t\right) + B'_i \sin\left(\omega_i t\right) \right] \right\}^2 \tag{3}$$

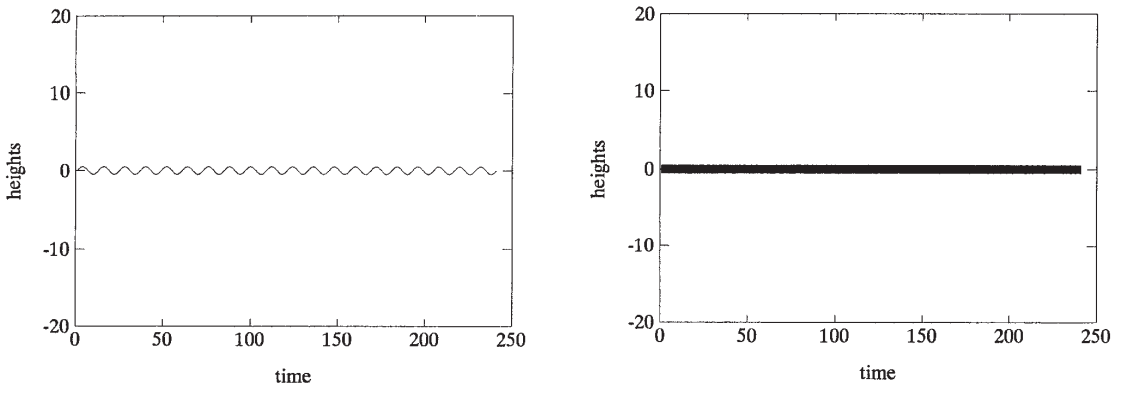

Fig. 1 - The pen-stroke effect - a real signal (left) with amplitude less than the pen stroke is not observed by the instrument (right).

where ε_a is the error in the approximation and $\varepsilon_a \neq \varepsilon_t$; $\forall$ t.

It follows by substituting Eq. (1) into Eq. (3) that

$$\varepsilon_a = 1/(N+1) \sum_{t=0}^{N+1} \left\{ X'_t + \varepsilon_t - \sum_{i=1}^{K} \left[A'_i \cos(\omega_i t) + B'_i \sin(\omega_i t) \right] \right\}^2 \tag{4}$$

and by applying the least square procedure to Eq. (3) the constants A'_i and B'_i are obtained, so that $H_i = (A_i^2 + B_i^2)^{1/2}$ and $\phi_i = \tan^{-1}(-B_i/A_i)$ are the amplitudes and phases of the Fourier components. The A'_i and B'_i are chosen by a least squares procedure so that

$$\left. \begin{array}{l} \lim \varepsilon_a \\ N \to \infty \end{array} \right\} \Rightarrow 0 \tag{5}$$

whatever the values of ε_t relative to X'_t, relative to the harmonic signal.

In this work, special attention is given to the measurement errors in X_t as part of ε_t. It must be noted that the approximation error ε_a is different from ε_t, and it is also treated here. The main measurement errors for a typical float tide gauge with a paper recording device, driven by an ordinary clock, are due to the clock mechanism, errors in measuring the heights and in time sampling. The major longest tidal records were produced with such devices, making the present analyses necessary for understanding their inbuilt measurement errors present in ε_t.

The determinations of lower limits for accepting tidal constants are examined by using rejection criteria that include the measurement errors. For instance, these devices use a pen to record sea-level heights. In this way, Fig. 1 is very instructive: no waves less than one pen stroke can be observed by the tidal gauge; thus, they cannot be present in the data set. Obviously, no constituents less than this limit can be obtained by tidal analysis, and, if they are, they deserve another interpretation.

2. Methods

2.1. Measurement errors due to clock and recording devices

In order to verify the importance of measurement errors in tidal analysis, a short real sea-level record from Cananéia, Brazil, was chosen and assumed free of errors (EFS), and synthetic series were produced from it containing:

a) errors due to a slow clock: ESC series,

b) errors in height sampling: EHS series,

c) errors due to jittered sampling: EJS series.

They were all Fourier analyzed and compared with the analysis of the error-free series EFS. The comparison was based on the Fourier estimates of A_i and B_i as given by solving Eq. (2), and the results were inferred as if they were tidal constituents, with H_i and ϕ_i calculated for a known estimated variance σ^2.

3. Results

3.1. Synthetic series with clock errors (ESC)

Fig. 2 (bottom) shows an example of a tide record when the clock of the tide gauge is slow, thus using a smaller amount L' of the recording paper, compared with the length of exact recording L (middle). During the recording period, the gauge continuously sampled the sea-level, but with an incorrect recording speed.

If $r_e = dl/dt$ is the exact recording speed, and dl is the length of the used paper during a time interval dt, $r_w = dl'/dt$ is the wrong recording speed, where dl' is the paper length used during the time interval dt. Since $dt = dl/r_e = dl'/r_w$, then

$$dl' = dl\, r_w / r_e \tag{6}$$

Fig. 2 also shows, at top, the case of a fast clock, where a greater amount of paper is necessary, and the new sampling interval is also given by an equivalent form of Eq. (6).

Synthetic series were produced for both cases, (slow and fast clock), by taking the digitized values of the EFS at standard intervals dt and attributing to them, in each case, a time interval dt' such that $dt'/dt = dl'/dl$, so that

$$dt' = dl'\, dt / dl \tag{7}$$

For the particular case of a tide gauge, with dt =1 hour and dl =1 cm, it follows from Eq. (7) that $dt' = dl'$ hour/cm, and $dt' = dl\, r_w/r_e$ hour/cm. But r_e = 1 hour/cm, thus

$$dt' = dl\, r_w \tag{8}$$

For a fast clock, $r_w > r_e$, so that $dt' > dt$; for a slow clock, $r_w < r_e$ and $dt' < dt$. The synthetic series were digitized at a standard interval Δt and Fourier analyzed. From the above relations and

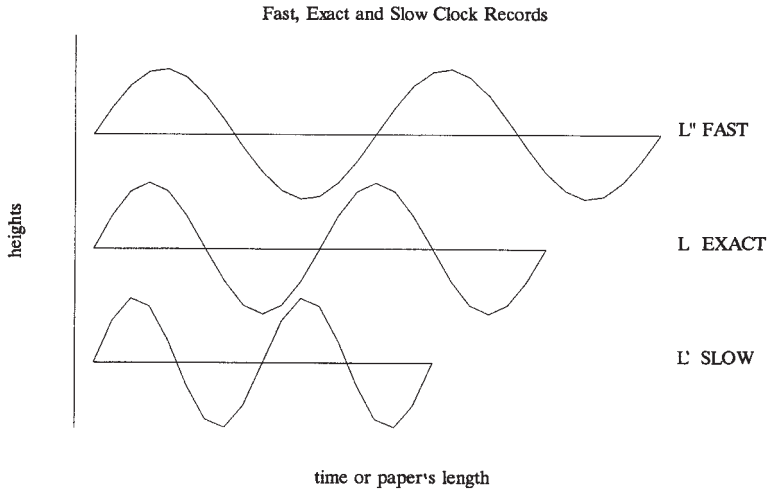

Fig. 2 - Hypothetical tidal record with clock errors - the case of a fast clock (top) uses more paper (L") to record the same tidal cycle than the exact clock (L, middle). A slow clock (bottom) uses less paper L'.

Fig. 2, for slow clock, it follows that $dt' = dt\ dl'/dl$, then

$$\Delta t' = (L'/L)\Delta t \tag{9}$$

A Fourier interpolation method is here used to correct for these errors from a slow clock series (ESC). A new series, named the Fourier Interpolated Series (FIS) is produced, and the estimated σ^2 is determined by comparing the Fourier amplitudes and phases of the FIS and EFS series. The interpolated values can be obtained by calculating the Fourier series at the instants $\Delta t' = j\Delta t$, j=1,2,....,N, where N is the number of observational 'points' in the EFS; so that $L/\Delta t = N$. For a fast clock, the interpolated series can be calculated in a similar way as in Eq. (9).

Fig. 3 shows the results of a comparison between the EFS and the slow clock series (ESC). As can be seen, there are differences of up to ±5 cm between the EFS and the ESC, with σ^2= 3.21 cm^2.

The results of the analysis of the FIS series, obtained by Fourier interpolation from the ESC series will be discussed in section 4.

3.2. Synthetic series with height sampling errors (EHS)

The second kind of measurement error in the analysis is examined by taking the error-free series, EFS, producing a synthetic series by adding to it artificial errors in the sea-level heights ε_t = ±1 cm, giving rise to the EHS, a series with known height errors. Both series are Fourier analyzed and the differences in amplitudes and phases were compared taking into account the artificially introduced errors.

The Fourier components of a time series that follows a mixed model, Eq. (1), when sampled from N observations X_1,..., X_N, may be written as the periodogram $I_N(\omega)$, where $-\pi < \omega < \pi$,

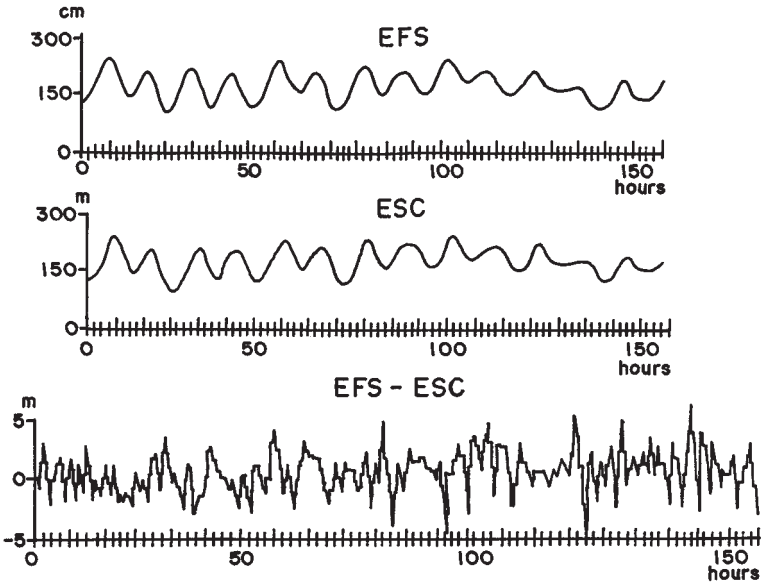

Fig. 3 - The error-free series (EFS), top, and the series with errors due to a slow clock (middle) have differences of up to ±5 cm (bottom).

(Priestley, 1981) such that

$$I_N(\omega) = 2 / N \left| \sum_{t=0}^{N} X_t \exp(-i\,\omega\, t) \right|^2 \tag{10}$$

This can be written for each ω in the equivalent form

$$E\left(I_N(\omega)\right) = 2 \sum_{s=-(N-1)}^{N+1} E\left(R(s)\right) \cos \omega\, s \tag{11}$$

where $E(R(s))$ is the expected value of the sample autocovariance function $R(s)$, so that $E(R(s))= (1- s /N)\ R_x(s)$, and thus

$$E\left(I_N(\omega)\right) = 2 \sum_{s=-(N-1)}^{N+1} (1 - s / N)\, R_x(s) \cos \omega\, s \tag{12}$$

where $R_x(s)$ is the theoretical autocovariance function of X_t such that

$$R_x(s) = R_z(s) + R_\varepsilon(s) = 1/2 \sum_{i=1}^{K} H_i^2 \cos \omega_i\, s + 2\delta_{0,\sigma} \tag{13}$$

where $R_\varepsilon(s) = 2\delta_{0,\sigma}$ is the autocovariance function of ε_t, so that $2\delta_{0,\sigma} = 1$ if $s = 0$, and $2\delta_{0,\sigma} = 0$ if σ is not equal zero.

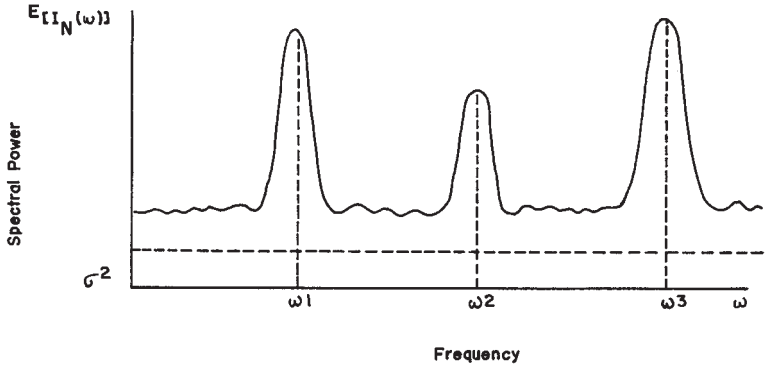

Fig. 4 - The form of the estimated periodogram may be visualized by superimposing Fejer Kernels centered on the frequencies ω_i.

From Eqs. (1), (10), (11), (12) and (13), one obtains

$$E\left(I_N(\omega)\right) = \sum_{i=1}^{K} H_i^2 \left(\sum_{t=0}^{N+1} (1 - s/N) \cos \omega_i s \cos \omega s \right) + 2\sigma^2$$

$$= \sum_{s=-(N-1)}^{K} H_i^2 \left(1/2 \sum_{t=0}^{N+1} (1 - s/N) \left\{ \cos\left[(\omega - \omega_i) s \right] + \cos\left[(\omega_i - \omega) s \right] \right\} \right) + 2\sigma^2 . \tag{14}$$

But,

$$\sum_{s=-(N-1)}^{N+1} (1 - s/N) \cos s\theta = (1/N) \left[\sin^2 (N\theta/2) \, \sin^2 (\theta/2) \right] = F_N(\theta) \tag{15}$$

where $F_N(\theta)$ is known as the Fejer Kernel. Writing Eq. (14) in terms of the Fejer Kernel gives

$$E\left(I_N(\omega)\right) = \sum_{i=1}^{K} H_i^2 \left((1/N) \left\{ \sin^2 \left[(\omega + \omega_i) N/2 \right] / \sin^2 \left[(\omega + \omega_i)/2 \right] \right\} + \right.$$

$$\left. + (1/N) \left\{ \sin^2 \left[(\omega - \omega_i) N/2 \right] / \sin^2 \left[(\omega - \omega_i)/2 \right] \right\} \right) + 2\sigma^2 . \tag{16}$$

The form of $E(I_N(\omega))$ may be visualized by superimposing 2K Fejer Kernels centered on the points $\omega \pm \omega_i$, $i = 1, ..., K$, with the constant interval $2\sigma^2$, as in Fig. 4.

It is well known that the expected value of the periodogram is directly related to the constituent amplitudes through

$$E\left(I_N(\omega)\right) \propto H^2(\omega). \tag{17}$$

Then, from Eqs. (15), (16) and (17), one can write

$$E\left(I_N(\omega)\right) = F_N(\theta) + 2\sigma^2; \tag{18}$$

and

$$H^2 = (1/c)^2 E\left(I_N(\omega)\right) = (1/c)^2 \left(F_N(\theta) + 2\sigma^2\right) \tag{19}$$

where $(1/c)^2$ is a constant of proportionality in Eq. (17). Therefore

$$(c\,H) = H' = \left(F_N(\theta) + 2\sigma^2\right)^{1/2}. \tag{20}$$

Now, expanding the R.H.S. of Eq. (20) as a Maclaurin series, with H>0, so that the amplitudes have only real and positive values that make physical sense, then $F_N(\theta)$> 0 and σ^2>0. $F_N(\theta)$ is a continuous and derivable function, and σ^2 is a positive number, it follows that

$$f(x) = (x+a)^n = a^n + n\,a^{n-1}\,x + n(n-1)a^{n-2}\,x^2/2! + n(n-1)(n-2)a^{n-3}\,x^3/3! + \ldots\ldots + P_s \tag{21}$$

Making $f(x) = H' = (F_N(\theta)+2\sigma^2)^{1/2}$, with $x = F_N(\theta)$, $n = 1/2$, $a = 2\sigma^2$, and using Eq. (21), it follows that

$$H' = H_0 + \left(2\sigma^2\right)^{1/2} \tag{22}$$

where $H_o = f(F_N(\theta))$, and then

$$H' = n a^{-1/2} F_N(\theta) + n(n-1)a^{-3/2}F_N^2(\theta)/2! + n(n-1)(n-2)a^{-5/2}F_N^3(\theta)/3! + \ldots\ldots + P_s \tag{23}$$

thus:

$$H' = H'' \pm \sqrt{2}\,\sigma = f\left(F_N(\theta)\right) \pm \sqrt{2}\,\sigma. \tag{24}$$

As one can see from Eq. (24), the amplitudes have an uncertainty interval, due to the error's variance, equal to $\pm\sqrt{2\sigma}$, to the first order, as shown in Fig. 5.

As N increases, the values of the Fejer Kernels sharpen towards the frequencies ω_1, ω_2 and ω_3, i.e., the truncation effects of the series are minimized by increasing the number of observations X_1,..., X_N. The uncertainty band around the periodogram of Fig. 4 is related to σ^2, which could be due to the error's variance, and does not diminish as N increases.

Values of $E(I_N(\omega))$ estimated as frequencies ω_1, ω_2 and ω_3, by discrete Fourier analysis, have the added contribution of the broader band defined in Eq. (16) by the error's variance. This will happen whenever $\omega = \omega_i = 2\pi/N$, $I = 0, 1, \ldots, N/2$, which is here assumed in order to simplify the description.

3.3. Synthetic series with errors due to jittered sampling (EJS)

This sort of error in the analysis is examined by taking the real tidal record as the error free series (EFS), $\{X_t\}$. A synthetic series is produced from the EFS record by additive sampling at instants:

$$s\,\Delta t_n' = \tau_n = n\,\Delta t \pm \varepsilon_t \tag{25}$$

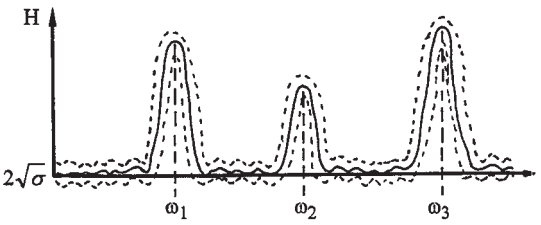

Fig. 5 - The uncertainty interval (first-order approximation) of the spectrum due to the error variance.

where n is an integer, Δt is the correct time interval and $\{\varepsilon_t\}$ are randomly distributed errors, so that

$$\left(\Delta t_n'\right) = \left(\tau_{n+1} - \tau_n\right) + \varepsilon_t \tag{26}$$

and

$$\Delta t'_{k+n} - \Delta t_n' = \left(\tau_{k+n} - \tau_n\right) + k\,\varepsilon_t. \tag{27}$$

Denoting by $P_k(\Delta t')$= Prob$[(\Delta t_k'-\Delta t_o) < \Delta t]$, the integrated probability function of the sampling interval being smaller than the correct sampling interval Δt, and the autocovariance function of $\{X(t)\}$ by

$$R(s) = E\left[X(t+s), X(t)\right] \tag{28}$$

the estimated autocovariance of the EJS can be obtained (Akaike, 1960) as

$$\rho(k) = \int R(\Delta t')\; dP_k(\Delta t') \tag{29}$$

where $\rho(k)$ is the jittered autocovariance function and $dP_k(\Delta t')$ is the derivative of the integrated distribution function of $P_k(\Delta t')$.

Taking $F(\omega)$ as the integrated spectrum of $\{X(t)\}$ and recalling that

$$R(\Delta t') = \int \exp\left(2\,\pi\, i\,\omega\,\Delta t'\right)\; dF(\omega) \tag{30}$$

it follows from Eq. (29) that

$$\begin{aligned} \rho(k) &= \int_{\Delta t'} \int_{\omega} \exp\left(2\pi i\;\omega\Delta t'\right) dF(\omega)\, dP_k(\Delta t') = \\ &= \int_{\Delta t'} \left[\int_{w} \exp\left(2\pi i\;\omega\Delta t'\right) dP_k(\Delta z')\right] dF(\omega). \end{aligned} \tag{31}$$

Thus

$$\rho(k) = \int_{\omega} \psi_k(\omega)\, dF(\omega) \tag{32}$$

where

$$\psi_k(\omega) = \int_{\Delta t'} \exp\left(2\pi i\;\omega\Delta t'\right) dP_k(\Delta t'). \tag{33}$$

This is the virtual transform of $dP_k(\Delta t')$ and is called characteristic function $\Psi_k(\omega)$.

For additive random sampling, the relation between the integrated spectrum $F(\omega)$ and its jittered form $F_j(\omega)$ can be expressed (Akaike, 1960; Shapiro and Silverman, 1960) as the Fourier transform of Eq. (32):

$$F_j(\omega) = (1/2\pi) \sum_{k=-\infty}^{\infty} \exp(-i\,\omega\,k)\rho(k). \tag{34}$$

So that the jittered spectrum $F_j(\omega)$ is positive and exists throughout the interval [-π,π], except for ω =0, where $F_j(\omega)$ becomes indeterminate (subscript *j* indicating jittered).

Another class of jittered spectra can be obtained for additive sampling from the characteristic function of the cumulative probability $P_k(\Delta t')$.

It was shown by Shapiro and Silverman (1960) that the additive random sampling is alias-free if the characteristic function $\Psi(\omega)$ is monotonic on the real axis for any *k* value. Cases corresponding to the "Poisson sampling" have the characteristic function

$$\psi(\omega) = \Gamma / (\Gamma - i\,s) \tag{35}$$

where Γ is the average rate of the Poisson process, and *s* a complex number. Eq. (35) takes one value on the real axis only, and the resulting jittered spectrum is alias-free. In general, when $\alpha \geq 0$, any function of the form

$$P(\Delta t') = \int_0^{\infty} P(\alpha, \Delta t')\, d\Theta(\alpha) \tag{36}$$

where Θ(α), the probability distribution function, is a decreasing function with a decreasing cosine transform such that

$$\int_0^{\infty} \Delta t'\; P(\Delta t')\, \delta\Delta t' = \int_0^{\infty} h(\alpha) d\Theta(\alpha) < \infty \tag{37}$$

with

$$\int_0^{\infty} \Delta t'\; P(\alpha, \Delta t')\, d\Delta t' = h(\alpha). \tag{38}$$

The continuous parameter $\alpha \geq 0$ indexes the integral of the probability densities $P(\alpha,\Delta t')$, and produces alias-free spectra. Thus, many sampling procedures can be constructed so that the aliasing is minimized for tidal analysis, and the amplitudes of the tidal constituents can be estimated with better accuracy.

3.4. Time sampling in practice

Time sampling errors are a common type of error in tide recording. The recording paper is loaded daily in the drum with a variable shifted position $\pm\Delta\chi$, which corresponds, depending upon the speed of the clock, to a time uncertainty of

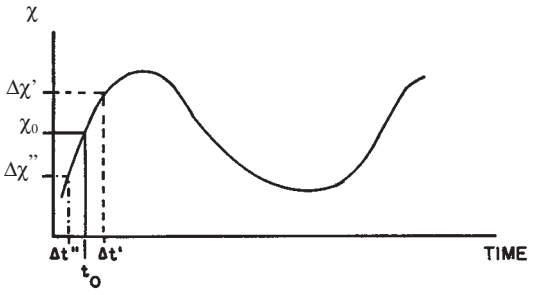

Fig. 6 - Uncertainties in time (Δt) and height (Δχ) around the point [t_0; χ_0] due to the digitization procedure.

$$\pm\Delta t' = \pm\Delta\chi / r_e \tag{39}$$

where r_e is the exact recording speed with which data are digitized. As depicted in Fig. 6, this will correspond to digitized uncertainties $\pm\Delta\chi$ in tidal heights. Also, these uncertainties introduce variabilities in phase, $\pm\Delta\phi$, relative to the pair [t_o, χ_o].

Values of $\Delta\chi$ are however generally asymmetrical about χ_o, although corresponding to symmetrical values $\pm\Delta t'$ relative to t_o. Direct symmetry only occurs when there is a linearity in tidal variability. Another aspect is that depending upon how sharp is the variability of the tide, values of χ ' and χ " can be of variable magnitude for the same $\pm\Delta t'$. These uncertainties will add to those errors described in the previous sections as errors in the amplitudes, and will contribute to the values of the tidal constituents.

The phase errors due to timing errors in the harmonics of expression in Eq. (1) may be estimated from

$$\pm\Delta\phi = \omega(\pm\Delta t') = \omega(\pm\Delta\chi) / r_e = 2\pi(\pm\Delta t') / T. \tag{40}$$

Thus,

$$\pm\Delta\phi = 2\pi(\pm\Delta t' / T) = \pm\Delta\tau 2\pi \tag{41}$$

where T is the period of the tidal component, $\Delta\tau = \Delta t' / T = \Delta\chi / r_e$, and ω is the frequency ($1/T$). Writing Eq. (41) in terms of $\omega_i = 2\pi p_i / N$ one obtains

$$\pm\Delta\phi_i = 2\pi(\pm\Delta t' / T_i) = \omega_i(\pm\Delta t') = 2\pi p_i(\pm\Delta t') / N \tag{42}$$

where p_1, p_2,..., p_k are integers so that $0 < p_i < N/2$, and N is the number of sampling values of χ. The larger ω , the larger is the uncertainty $\pm\Delta\phi_i$ for a given $\pm\Delta t'$.

4. Discussion and conclusions

Classical approaches to the problem of estimating the uncertainties in tidal constituents were illustrated by Munk and Cartwright (1966) and Franco and Rock (1974), so that the weaker lines

in the mixed spectrum of Eq. (1) could be objectively described, and disregarded or accepted.

The probability distribution of $|Z(\omega)|$ and $\phi_z(\omega)$ of the transfer function were calculated as:

$$\left|Z(\omega)\right| = F\chi(\omega) / G(\omega) \tag{43}$$

where $F\chi(\omega)$ is the Fourier transform of the tidal record, and $G(\omega)$ the time correspondent Fourier transform of the tide generating potential, and $\phi_z(\omega)$ are the phases of $Z(\omega)$.

Franco and Rock (1974) arrived to nearly the same probability distribution and proposed a criterion for rejecting the weaker lines of the tidal spectrum.

In both approaches, it was considered that the limiting level in the precision of any tidal analysis is not the accuracy of the measurement but the amount of noise present in the tidal record. Eq. (4), which gives the approximation error ε_a, shows that for stationary process the values of A'_i and B'_i are determined, so that $\varepsilon_a \rightarrow 0$. This means that both X'_t (the harmonic signal of X_t) and ε_t, the total error associated with the signal, can be approximated by A' cos $\omega_i t$ and B' sin $\omega_i t$ with that accuracy.

So, whatever ε_t, including any uncorrelated signal, it will be represented by A' cos $\omega_i t$ and B' sin $\omega_i t$; in that respect, ε_a will tend to zero ($\varepsilon_a \rightarrow 0$), but ε_t will not.

Gutièrrez et al. (1981), studied the indetermination of the tidal harmonic constants, concluding that tidal constants cannot be considered as "constant" constants, and improving the analyses using high resolution filter procedures.

Mosetti and Purga (1985) also discussed some questions on the reliability of the analysis of tides and related phenomena, concluding that the use of high resolution filter procedures improves the analyses by filtering the non tidal signals present in a sea-level record.

Mosetti (1983) arrived at similar results by using a Kalman filter estimate of the tidal harmonic constants. It was pointed out in this work the importance of assuming that the tidal harmonic constants are random variables.

All these works deal with the minimization of the approximation error ε_a, obtaining highly accurate results on the determination of tidal constituents. The success of these methodologies is related to the high efficiency of the used filtering procedures, which can eliminate variabilities due to meteorological effects and other non-linear signals present in the sea-level record. Gutièrrez et al. (1981.), Mosetti and Purga (1985), and Mosetti (1983) proved that the amount of geophysical noise present in the tidal record can be minimized using adequate mathematical procedures.

In the present work, the impossibility of disregarding the measurement errors present in ε_t, that will never be eliminated by mathematical procedures, is discussed. The design of objective criteria for rejecting the weaker lines of tidal spectrum based on the accuracy of the measurement is also a matter of concern.

4.1. Comparison of analysis of EFS and FIS

The interpolated series described in connection to synthetic series with clock errors were Fourier analyzed. The original series (EFS), its corresponding slow clock series (ESC), and the

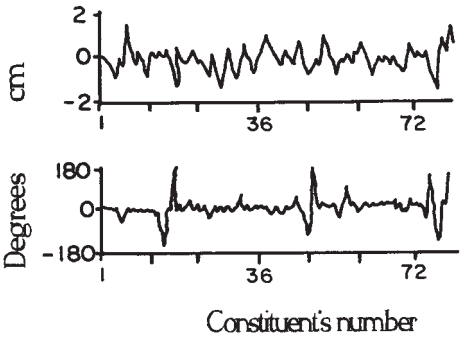

Fig. 7 - Amplitude (top) and phase differences (bottom) between the FFT analysis of the error-free series (EFS) and the Fourier interpolated series (FIS).

differences, are shown in Fig. 3. The differences between them have absolute maxima of |5 cm|. The ESC series was corrected, as explained in section 3, to give the Fourier Interpolated Series (FIS).

The corresponding differences in the spectra of the EFS and FIS are shown in Fig. 7. As can be seen, the differences in amplitude are well within |2 cm|, and the phases differences are nearly zero, except for a few values. Bearing in mind that typical values for the error were about $\Delta\chi=\pm1$ cm and $\sigma\approx1$, it can be assumed that the expected error of the analysis will be about $\sqrt{2} = 1.41$ cm. This value is well comparable to the differences in amplitude of Fig. 7, showing that the Fourier Interpolation to correct series with clock errors is quite acceptable.

Another use of the interpolation method is in completing series with less data points than a power of two, so that they can be analyzed by FFT procedures. The results are nearly identical to using the normal procedures, but with much less computational time (Franco, personal communication).

4.2. Comparison of EFS and EHS analyses

Comparative Fourier analysis of the EFS and EHS series was done in such a way that the truncation errors are equally displayed by both series. In fact, from Eqs. (16) and (22) it follows that

$$E\left(I_N(\omega)\right)_{EFS} - E\left(I_N(\omega)\right)_{EHS} = 2\sigma^2 \tag{43}$$

where σ represents the variance of the total error.

Estimates of $\phi(\omega)$ for both series were calculated from $I_N(\omega)_{EFS}$ and $I_N(\omega)_{EHS}$, and the differences calculated from

$$\phi(\omega) = \left[\left(I_m\, I_N(\omega) / R_\varepsilon\, I_N(\omega)\right)_{EFS} - \left(I_m\, I_N(\omega) / R_\varepsilon\, I_N(\omega)\right)_{EHS}\right]. \tag{44}$$

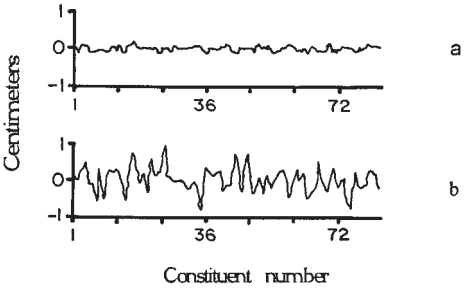

Fig. 8 - Spectral differences in the amplitudes of the error-free series (EFS) and two series with height errors (EHS) - a) random errors distributed continuously over the interval [-1;1]. b) integer errors (+1 or -1) randomly added to the EFS to produce the EHS.

Values of $\phi(\omega)$ correspond to the variance limits σ^2. Figs. 8 and 9 show the values of Eqs. (43) and (44) for case a) random errors $\Delta\chi$, distributed continuously over the interval [-1,1], added to the EFS to produce the EHS series. Case b) corresponds to the EHS series but with random errors $\Delta\chi$=±1, (integer values).

As shown in all Figs., the amplitude differences $\Delta H(\omega)$ as a function of ω follow Eq. (24) by showing σ^2= 0.99 for case b), which represents the error normally generated in the process of tidal data reduction. For its part, the mean value of the phase differences $\Delta\phi(\omega)\approx 3°$ with a standard deviation of 54°, also shows that tiny errors in heights may introduce major errors in the phase determinations. Figs. 10 and 11 display the values of $\Delta H(\omega)$ against the amplitudes $H(\omega)$, as given by the analysis of the EFS; the $\Delta\phi(\omega)$ values are also shown against the amplitudes $H(\omega)$ of the Fourier components. Values of $\Delta H(\omega)$ are well-distributed from -1 to 1 cm, and nearly independent of $H(\omega)$; for phases, $\Delta\phi(\omega)$ values start to be well scattered over the interval [-180°,180°] for amplitudes $H(\omega)$ < 5cm. For values $H(\omega)$ > 5 cm, though the phase differences $\Delta\phi(\omega)$ seem nearly equal to zero.

From Eq. (1), if $X'_t << \varepsilon_t$, then $X_t = X'_t + \varepsilon_t \approx \varepsilon_t$, and X'_t cannot be assessed. Under this circumstance, ε_a given by Eq. (4) will tend to zero, and $X'_t \,\forall\, t$ will not be measured. Thus, the minimum spectral amplitude to be registered from Eqs. (16) and (22) is $\Delta H' = \sqrt{2\sigma} \approx 1.41\text{cm}$, for

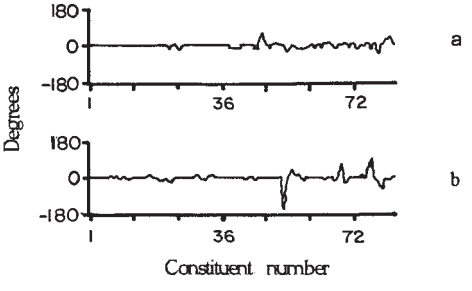

Fig. 9 - Spectral differences in the phases of the error-free series (EFS) and two series with height errors (EHS) -a) random errors distributed continuously over the interval [-1;1]. b) integer errors (+1 or -1) randomly added to the EFS to produce the EHS.

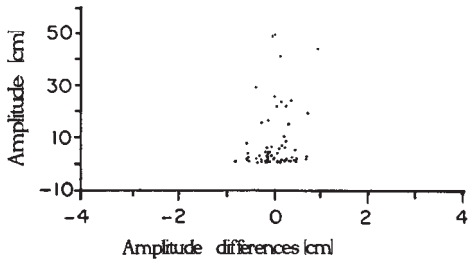

Fig. 10 - Distribution of the amplitude differences ΔH(ω) against the error-free amplitudes for case b of the EHS.

σ= 1 cm, which is followed for the above comparisons.

4.3. Comparison of the analyses of EFS and EJS

The EFS and EJS were compared and the results are show in Fig. 12. As expected, differences in amplitudes of the periodogrammes of the series are within the limits ±1 cm, while variations of ϕ_i differences in phase are smaller for low than for high frequencies. The distribution of these differences plotted against the amplitudes of the EFS constituents are shown in Fig. 13 for phase differences, and in Fig. 14 for amplitude differences. For small amplitudes, the differences in amplitudes ΔH_i and phases $\Delta\phi_i$ are larger. In general, the smaller amplitudes of the spectra are associated with the higher frequencies, and so the spreading of the $\Delta\phi_i$ values at low amplitudes in Fig. 12 is due to timing errors introduced, really, in the supposed error-free series EFS.

No values at low frequencies were higher than 1 cm or smaller than -1 cm in ΔH_i, suggesting that no aliasing was introduced by the additive random sampling procedures, an advantage from the point of view of the analysis. However, this advantage is not maintained in the phases which were not improved at higher frequencies and degraded the calculation. The general results show that the amplitudes may be calculated alias-free from an adequate jittered sampling scheme, and the phases will be spoiled by the process, especially at higher frequencies.

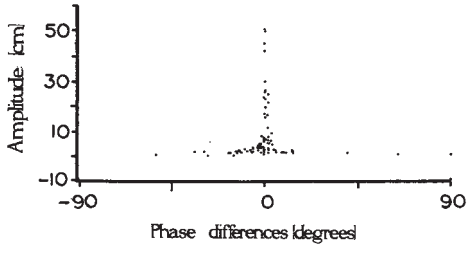

Fig. 11 - Distribution of the phase differences Δϕ(ω) against the error-free amplitudes for case b of the EHS.

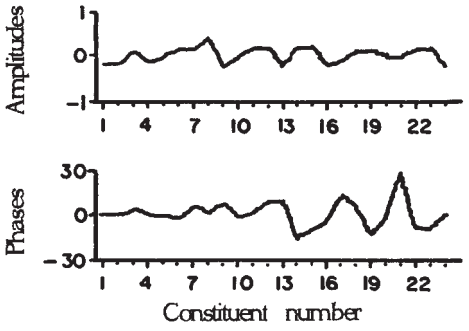

Fig. 12 - Spectral difference for amplitudes (top) and phases (bottom) between the error-free series (EFS) and the series with jittered sampling (EJS).

4.4. Final outcomes

It was shown that measurement errors cannot be minimized by mathematical procedures, making the weaker lines of the spectrum with amplitudes less than $\sqrt{2}\sigma$, where σ is the standard deviation of the measurement errors, unassessable. Further, the phases of these components may be badly determined whatever the correcting method used, so that the tidal constants, particularly at higher frequencies, may no longer be taken as (constant) constants.

The use of filtering procedures to "clean" the sea-level record diminishes the approximation error ε_a, but no mathematical procedure exists to obtain a signal that was not measured, as depicted in Fig. 1.

Fourier interpolation is shown to be an adequate technique to recover the original series spoiled by a slow or fast clock recording.

Jittered sampling may be used to one's advantage in tidal analysis to minimize aliasing; in spite of this, the phases of the constituents are not improved with the process.

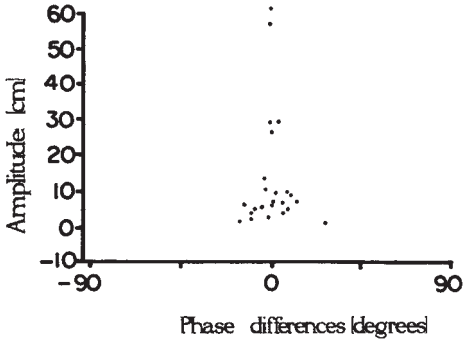

Fig. 13 - Distribution of the spectral differences in the phases of the error-free series (EFS) and the series with jittered sampling (EJS).

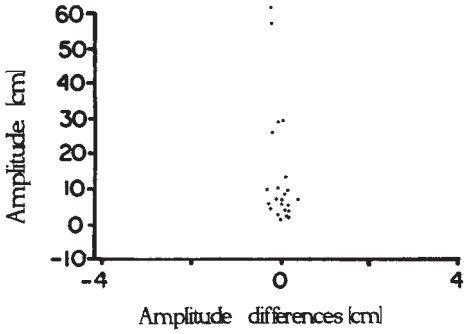

Fig. 14 - Distribution of the spectral differences in the amplitudes of the error-free series (EFS) and the series with jittered sampling (EJS).

Acknowledgments. We are grateful to Prof. Pedro Alberto Morettin for helpful discussions, and also to MSc. Carlos Augusto de Sampaio Frana, and BSc. Josè Claro da Fonseca who did the drawings. Also, E. Marone thanks the International Centre for Theoretical Physics, Trieste, Italy, where the paper was partially prepared during associate visits.

References

Akaike H.; 1960: *Effect of timing error on the power spectrum of sampled data,* In: Suetura Z., Aoyama H., Hayashi C., and Matusita K. (eds), Annals of the Institute of Statistical Mathematics, **11**, pp. 145 - 165.

Cartwright D. E. and Amin M.; 1988: *The variances of tidal harmonics.* Dt. hydrogr. Z., **39**, 235-253.

Franco A. S. and Rock N. J.; 1974: *Comparative accuracy of Fourier tidal analysis employing different time spans with reference to a Doodson analysis.* Ciência e Cultura, **26**, 498-507.

Gutièrrez A., Mosetti F. and Purga N.; 1981: *On the indetermination of the tidal harmonic constants.* Nuovo Cim., **4C**, 563-575.

Marone E.; 1991: *Processamento e análise de dados de maré. Discurso dos métodos.* PhD. Thesis. Instituto Oceanográfico da Universidade de São Paulo. São Paulo, Brazil, 232pp.

Mosetti F. and Purga N.; 1985: *Some questions on reliability of the analysis of tides and related phenomena.* Boll. Geof. Teor. Appl., **3**, 219-253.

Mosetti R.; 1983: *A Kalman-Filter Estimate of the Tidal Harmonic Constants.* Nuovo Cim., **6C**, 445-452.

Munk W. H. and Cartwright D. E.; 1966: *Tidal Spectroscopy and prediction.* Phil. Trans. Roy. Soc. A, **1105**, 533-581.

Priestley M. B.; 1981: *Spectral Analysis and Time Series.* Academic Press, London. 890 pp.

Shapiro H. S. and Silverman R. A.; 1960: *Alias-free sampling of random noise.* Jour. Soc. Indust. Appl. Math., **8**, 225-248.

Zetler B. D., Cartwright D. E. and Berkman S.; 1979: *Some comparison of response and harmonic tide predictions. Int. hydrogr*. Rev., **56**, 105-115.